Structural Optimization For Flutter Instability Problems

Pedro André de Carvalho Pastilha

Instituto Superior Técnico,
October 2007

Abstract

The present work deals with the finite element analysis and optimization of structures for flutter instability originated by the action of non-conservative forces. Three models are considered for this purpose. The first case considers a cantilevered circular beam subjected to a partially non-conservative end-load, such as the thrust generated by a single propeller rocket. The second considers a thick plate subjected to the same type of end load as the circular beam. Finally the third model focuses on the problem of a flat panel subjected to the non-conservative load generated by a low supersonic flow. As a first optimization method, optimized designs are obtained by varying the column's cross-sectional area. In a later stage, plate element formulation is used to obtain different optimized structures for equivalent loading conditions. Considering this plate element formulation, optimized structures are also obtained for the case of the plate subjected to a supersonic flow. Results for the stability analysis and optimized results are presented and discussed for each model.

1 Introduction

In general terms, flutter is a dynamic instability of a body subjected to non-conservative forces wherein its oscillations increase without bounds. Hence, this is a serious concern when dealing with the design and project of any structure subjected to these forces. In aeronautical terms, flutter is an aeroelastic self-excited vibration with a sustained or divergent amplitude, which occurs when a structure is placed in a flow of sufficiently high velocity.

The present work deals with the stability analysis of simple structural elements subjected to non-conservative loads and subsequent optimization procedures in order to minimize structural volume while keeping stability conditions. There are several engineering areas in which non-conservative loads are quite common such as automotive, aeronautics or even space structures. For all these applications the importance of optimal designs is reinforced by the constant need of lighter structures with very high stability requirements.

As a first model considered in the present work, consider a single propeller rocket subjected to thrust and aerodynamic drag, both good examples of partial non-conservative forces. The concept of partial non-conservative force can be explained by considering the rocket propeller from the mentioned structure. While the thrust from the rocket engine is a pure non-conservative force (which may change in direction and magnitude with time and structural geometry variations), the weight of the engine itself is a conservative load (does not change direction or magnitude with time or structural displacement). This complex physical problem can be simplified to the case of a simple cantilevered column subjected to a partial non-conservative force as shown in Fig. 1. Despite generating some controversy (as discussed by Sugiyama et al. (2002); Langthjem et al. (1999); Elishakoff (2005)), the simplified model allows for insightful and more efficient analysis and optimization studies. In addition, the presented model shows equivalent stability characteristics as a full model and the results have been verified experimentally (by Sugiyama et al. (2000)).

When a structure is subjected to the combined action of both conservative and non-conservative forces, different instability modes need to be considered depending on the loading characteristics. The presented work shows that when a uniform cantilever column is subjected to a pure conservative load or when the non-conservative load contribution is relatively small (less than half of the total applied load), the instability mode presents itself as divergence. As the non-conservative load component increases (above half of the total applied load), instability occurs as flutter. Flutter instability can be defined as an unfavorable coupling between dynamic and static loads, which results in the loss of structural stability and, ultimately, structural collapse. The presented formulations developed follow the work by Langthjem and Sugiyama (1999,

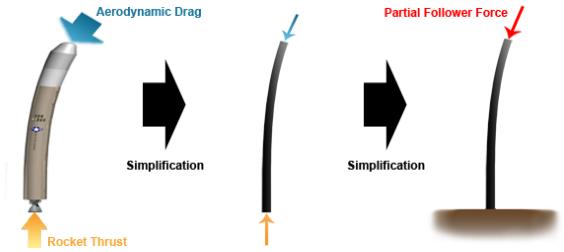

Figure 1: Assumed simplifications to establish the considered model.

2000a,b).

The differential equations describing the behavior of the presented model are solved using the finite element method and the stability conditions for the column are displayed as load-frequency curves. A first optimization process was implemented, consisting on the minimization of the structural volume by varying the cross-sectional areas of the column while maintaining the stability conditions above the values obtained for the uniform column. For this optimization process the column was modeled using bidimensional beam elements.

A second finite element model is considered for the same physical problem by using three-dimensional plate element. Stability results are presented for the uniform case, and a thickness optimization process is implemented in order to obtain new optimized designs. General studies of plates subjected to distributed follower loads are presented by Kim and Park (1998); Kim and Kim (2000) and Jayaraman and Struthers (2005). Zuo and Schreyer (1996) developed analysis techniques for divergence and flutter instability of beams and plates subjected to follower forces.

Using the same plate finite element formulation, the problem of a flat plate under a low supersonic flow is considered. The instability phenomenon that occurs in these conditions is called panel flutter and has been studied by Suleman and Venkayya (1994, 1996). Optimization studies for panel flutter have also been developed by Suleman and Gonçalves (1997) using piezoelectric patches and Odaka and Furuya (2005) presents a robust thickness optimization for a plate wing.

In order to maintain stability conditions for all the considered models, constraints had to be applied to the critical load values during the optimization process. To avoid large jumps in the critical load between the iterative steps of the optimization process, the frequency curves also required constraints. It is known that the stability conditions of a structure subjected to a non-conservative force may not evolve smoothly with small geometry changes. Therefore, the optimization process in these conditions becomes somewhat difficult and requires strong optimization algorithms based on sensitivity analysis in order to determine the derivatives of the objective and constraint functions with respect to the project variables. The optimization process was performed using the method of moving asymptotes developed by Svanberg (1987).

A more detailed description of the models presented and discussed in the present work can be found in the thesis work developed by Pastilha (2007).

2 Theoretical Models

2.1 Dynamic Stability of Elastic Columns Subjected to Non-Conservative Loads

The mathematical model that describes small amplitude vibrations on a cantilevered column following the Bernoulli-Euler beam theory takes the form,

$$\frac{\partial^2}{\partial x^2}\left(EI\frac{\partial^2 w}{\partial x^2}\right) + m\frac{\partial^2 w}{\partial t^2} + p\frac{\partial^2 w}{\partial x^2} = 0, \qquad (1)$$

where E is the elasticity modulus, $I = I(x)$ is the area moment of inertia, $m = m(x)$ is the mass per unit length, p is the load applied at the free end of the column and $w = w(x,t)$ is the transverse displacement at the instant t and at the position x. Considering that the load p has two components (conservative and non-conservative, the parameter η is introduced to define the fraction of the total applied load that is non-conservative, as represented in Fig. 2. For a clamped column at $x = 0$ and free at $x = L$, the boundary conditions are given by

$$\begin{aligned} w(x=0,t) = 0, \quad \frac{\partial w(x=0,t)}{\partial x} &= 0, \\ EI\frac{\partial^2 w(x=L,t)}{\partial x^2} &= 0, \qquad (2) \\ \frac{\partial}{\partial x}\left(EI\frac{\partial^2 w(x=L,t)}{\partial x^2}\right) + & \\ p(1-\eta)\frac{\partial w(x=L,t)}{\partial x} &= 0. \end{aligned}$$

Having defined the general equations which describe the behavior of the column, it is now possible to formulate the corresponding boundary value problem by considering that the displacements are given in the form,

$$w(x,t) = \tilde{w}(x)\exp(\lambda t), \quad \lambda = \alpha + i\omega \qquad (3)$$

and scaling the problem variables into a dimension-

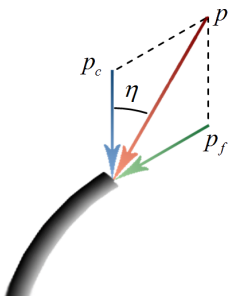

Figure 2: Graphical representation of the load parameter η.

less form as

$$\bar{x} = \frac{x}{L}, \quad \bar{w} = \frac{\tilde{w}}{L}, \quad \bar{p} = \frac{pL^2}{EI_0}, \quad \bar{m}(\bar{x}) = \frac{m(x)}{m_0}, \quad \bar{I}(\bar{x}) = \frac{I(x)}{I_0}, \quad \bar{t} = \frac{t}{L^2}\sqrt{\frac{EI_0}{m_0}}, \quad \bar{\lambda} = \frac{t}{\bar{t}}\lambda, \quad (4)$$

where the index '0' corresponds to a uniform column. Replacing these dimensionless quantities in equations 1 and 3, we have,

$$\begin{aligned} \frac{\partial^2}{\partial\bar{x}^2}\left(\bar{I}\frac{\partial^2}{\partial\bar{x}^2}\left(\bar{w}\exp\left(\bar{\lambda}\bar{t}\right)\right)\right) + \\ \bar{m}\frac{\partial^2}{\partial\bar{t}^2}\left(\bar{w}\exp(\bar{\lambda}\bar{t})\right) + \\ \bar{p}\frac{\partial^2}{\partial\bar{x}^2}\left(\bar{w}\exp\left(\bar{\lambda}\bar{t}\right)\right) &= 0, \\ \bar{w}(\bar{x}=0,\bar{t})=0, \quad \frac{\partial\bar{w}(\bar{x}=0,\bar{t})}{\partial\bar{x}} &= 0, \\ \bar{I}\frac{\partial^2\bar{w}(\bar{x}=1,\bar{t})}{\partial\bar{x}^2} &= 0, \\ \frac{\partial}{\partial\bar{x}}\left(\bar{I}\frac{\partial^2\bar{w}(\bar{x}=1,\bar{t})}{\partial\bar{x}^2}\right) + \\ \bar{p}(1-\eta)\frac{\partial\bar{w}(\bar{x}=1,t)}{\partial\bar{x}} &= 0. \end{aligned} \quad (5)$$

Having defined the dimensionless problem for the beam case the over bars will no longer be used, for notation simplicity. Although it is possible to obtain a semi-analytical solution for this problem, it is only valid for columns with constant mass and stiffness distributions. When considering a column with non-uniform sections, a discretization method is required in order to obtain the solution for these equations.

2.2 Dynamic Stability of Plates Subjected to Non-Conservative Loads

2.2.1 Dynamic Stability Analysis of a Cantilevered Plate Subjected to an End Load

In order to describe the deformations of a plate the First Order Shear Deformation Theory, also known as the Mindlin plate theory, is considered. This theory is set upon a displacement field given by (Reddy, 1992),

$$u_1 = u + z\varphi_x, \quad u_2 = v + z\varphi_y, \quad u_3 = w, \quad (6)$$

where (u, v, w) are the displacements of a point with coordinates $(x, y, 0)$ and φ_x and φ_y are the rotations of the transverse normal about the y and $-x$ axes, respectively. For a linear theory based on infinitesimal strains and orthotropic materials it is possible to demonstrate that the in-plane displacements (u, v) are uncoupled from the transverse deflection. The in-plane displacements are governed by plane elasticity equations and are not considered in the present work therefore only the equations governing the bending deflections $(w, \varphi_x, \varphi_y)$ are developed. For the considered model, represented in figure 3, a distributed load P is applied to the side of the plate opposite do the cantilevered face. This load has a conservative in-plane component N_c and a tangential component P_f, where the relative magnitude of each force is determined once again by the parameter η which is defined analogously to the the beam model as

$$\eta = \frac{P_f}{N_c + P_f} = \frac{P_f}{P}. \quad (7)$$

Following the assumptions stated by Mindlin, the strain energy for an isotropic shear deformable plate is given by,

$$\begin{aligned} U = \frac{1}{2}\int\int D\left[\left(\frac{\partial\varphi_x}{\partial x}\right)^2 + 2\nu\frac{\partial\varphi_x}{\partial x}\frac{\partial\varphi_y}{\partial y} + \right. \\ \left.\left(\frac{\partial\varphi_y}{\partial y}\right)^2 + \frac{1-\nu}{2}\left(\frac{\partial\varphi_x}{\partial y} + \frac{\partial\varphi_y}{\partial x}\right)^2\right] + \\ A\left[\left(\varphi_x + \frac{\partial w}{\partial x}\right)^2 + \left(\varphi_y + \frac{\partial w}{\partial y}\right)^2\right] dxdy, \end{aligned} \quad (8)$$

where D is the bending stiffness of the isotropic plate and A is the extensional stiffness. Likewise, the kinetic energy of the plate is,

$$\begin{aligned} T = \frac{1}{2}\int\int I_m\left[\left(\frac{\partial\varphi_x}{\partial t}\right)^2 + \left(\frac{\partial\varphi_x}{\partial t}\right)^2\right] + \\ m\left(\frac{\partial w}{\partial t}\right) dxdy, \end{aligned} \quad (9)$$

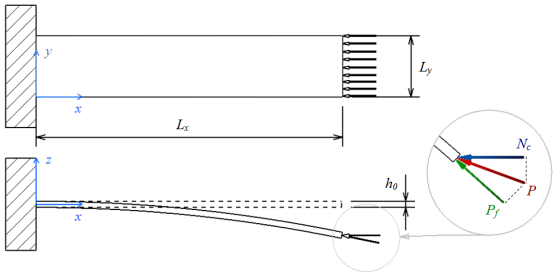

Figure 3: Geometric dimensions and load properties for the presented model.

where I_m corresponds to the mass moment of inertia and m is the mass per unit area of the plate. The potential energy corresponding to the conservative component of P is given by

$$V = \frac{1}{2}\int\int P\left(\varphi_x\right)^2 dxdy, \tag{10}$$

and the virtual work done by the nonconservative load can be obtained from,

$$\delta W_f = \int\int \eta P \frac{\partial w}{\partial x}\bar{\delta}(x-a)\delta w dxdy, \tag{11}$$

where $\bar{\delta}$ is the Dirac delta function. The equations of motion can now be derived from the previous equations using the generalized form of Hamilton's principle

$$\delta\int_{\bar{t}_1}^{\bar{t}_2}\left[T - U + V + W_f\right]d\bar{t}. \tag{12}$$

Assuming harmonic motion, the global displacement vector can be written as,

$$\mathbf{u} = \tilde{u}\exp(\lambda t), \quad \lambda = \alpha + i\omega, \tag{13}$$

Introducing the following dimensionless variables

$$\begin{aligned} \bar{x} = \frac{x}{L_x}, \quad \bar{y} = \frac{y}{L_x}, \quad \bar{w} = \frac{\tilde{w}}{L_x}, \\ \bar{P} = \frac{PL_x^2}{D_0}, \quad \bar{A} = \frac{Ah_0}{D}, \quad \bar{m}(\bar{x},\bar{y}) = \frac{m(x,y)}{m_0}, \\ \bar{I_m}(\bar{x},\bar{y}) = \frac{I_m(x,y)}{m_0 h_0^2}, \quad \bar{t} = \frac{t}{L^2}\sqrt{\frac{D_0}{m_0}}, \quad \bar{\lambda} = \frac{t}{\bar{t}}\lambda, \end{aligned} \tag{14}$$

where the index '0' corresponds to a plate with uniform thickness h_0. As for the beam model, the overbars denoting the dimensionless quantities will no longer be used for notation simplicity. By replacing these dimensionless quantities and the displacement vector defined by 13 into equation 12 it is possible to obtain the dimensionless equation that can be discretized from the finite element method.

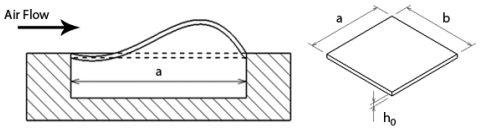

Figure 4: Simply supported plate under a Supersonic Flow.

2.2.2 Dynamic Stability Analysis of a Plate Under Supersonic Flow

Piston theory is an inviscid unsteady aerodynamic theory that is used quite often in supersonic and hypersonic aeroelasticity. With it, it is possible to determine a relationship between the local pressure on any point of the considered surface and the component of fluid velocity normal to the moving surface. The derivation of this expression utilizes the isentropic simple wave expression for the pressure on the surface of a moving piston, resulting in the following pressure difference distribution (Odaka and Furuya, 2005),

$$\Delta p = \frac{\rho_\infty U_\infty^2}{\sqrt{M_\infty^2 - 1}}\left(\frac{\partial w}{\partial x}\right), \tag{15}$$

where a zero flow deflection is assumed for the panel's leading and trailing edges and aerodynamic damping is ignored. The work done by the surface pressure resulting from the aerodynamic flow can be obtained from the principle of virtual work as,

$$\delta W_{pf} = \int\int \frac{\rho_\infty U_\infty^2}{\sqrt{M_\infty^2 - 1}}\left(\frac{\partial w}{\partial x}\right)\delta w dxdy. \tag{16}$$

The governing equation for a plate subjected to a supersonic flow is then obtained by replacing the term corresponding to the virtual work developed by the non-conservative end-load model in equation 12 with the work given by equation 16.

3 Finite Element Analysis

The discretization of the previously introduced differential equations and corresponding boundary conditions given in dimensionless form by equations 1 and 3 for the beam model and by equation 12 for the plate models, are solved using the finite element method. For the beam model, two node elements with two degrees of freedom at each node are considered with full integration. For the plate models, four node elements are considered with reduced integration and three degrees of freedom at each node. Reduced integration is used to minimize the effects of shear locking verified for thin plates. For the

beam case, the column is divided into N_e line elements, each with length l_e and a linear diameter variation given in element coordinates by,

$$h_e = (1 - \xi)\,\mu_e + \xi\mu_{e+1} \tag{17}$$

in which μ is the diameter of the beam at node e. For the plate discretization, the structure is divided into N_{e_x} elements in the x direction and N_{e_y} elements in the y direction, each with a length l_x and height l_y. The thickness distribution along the element is also assumed to have a linear evolution according to,

$$h_e = \sum_{i=1}^{4} \frac{1}{4}(1 + \xi\xi_i)(1 + \zeta\zeta_i)\mu_i, \tag{18}$$

given in the element local reference frame. Using Hermite cubic interpolation functions for the beam element discretization and Lagrange linear interpolation functions for the plate problems results in the following eigenvalue problem,

$$\mathbf{Lu} = \left[\mathbf{K} - \lambda^2\mathbf{M} - P\left(\mathbf{G_c} - \eta\mathbf{G_f}\right)\right]\mathbf{u} = 0, \tag{19}$$

where $\mathbf{K}$ is the stiffness matrix, $\mathbf{M}$ is the mass matrix, $\mathbf{G_c}$ and $\mathbf{G_f}$ are the load matrices corresponding to the conservative and non-conservative load components, respectively. These two last matrices are replaced by the dimensionless dynamic pressure loading matrix $\mathbf{Q}$ in the panel flutter problem.

The solution of equation 19 was implemented using $MATLAB^{®}$ and the solutions are obtained by defining a set of load points between 0 and p_{final} (Q_{final} for the panel flutter model) and extracting the corresponding frequency eigenvalues and eigenmodes for each of these loads. Several studies were developed to determine the adequate number of load points, to decide upon the value of p_{final} and to define the number of elements necessary to produce accurate results. A verification study was also developed for both finite element models, comparing some results from the implemented codes with results from the commercial software $ANSYS^{®}$. Results have shown a good agreement both for the beam and plate element codes.

3.1 Stability Results for a Column Subjected to a Partial Non-Conservative End Load

The solution for the eigenvalue and eigenvector problem presented by equation 19, for both the beam and plate problems subjected to non-conservative end loads, was implemented in $MATLAB^{®}$ in order to obtain the eigenvalue frequency and corresponding modes for any given load p. Evaluating these frequency values, it is possible to identify the loads for which the structure loses rigidity and the corresponding instability mode. For a given load parameter η, when a frequency reaches zero, the instability mode is divergence. Flutter occurs when two frequency values coalesce, resulting also in the loss of structural rigidity.

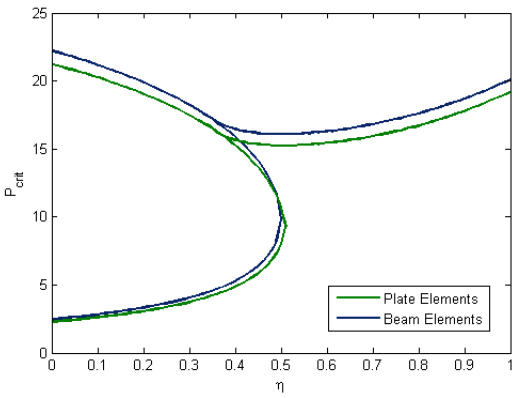

Figure 5: Stability diagram of the uniform plate, presenting also the results from the beam model.

The stability diagram presented in figure 5 shows the evolution of the critical divergence and flutter loads with different possible load conditions ranging from ($\eta = 0$ to $\eta = 1$), as was done before. The results obtained for the plate are presented along with the stability results obtained for the beam model. As it can be seen from the diagram, the instability mode changes from divergence to flutter at $\eta = 0.5$. From this diagram it is also possible to notice that as divergence turns into flutter, the stability margin also increases significantly. This is mainly because damping effects are not considered in the present analysis, although it can also be verified in a smaller degree for damped structures. Another conclusion that can be taken form the figure is that both the beam and plate models produce quite similar results, in spite of the critical loads for the plate model being generally inferior to the ones obtained from the beam model.

As mentioned earlier, flutter occurs when frequency coupling is verified at any given load condition. Thus, one of the most important analysis aspects to consider when studying this type of instability problems is the structural load-frequency response. Figure 6 shows the frequency load curves of a uniform column with a load parameter of $\eta = 0.5$, representing both the real part of the frequency and the imaginary part. This load condition was chosen because at this load condition the main instability mode changes from divergence ($\eta < 0.5$) to flutter ($\eta > 0.5$). As the image shows, the critical load for the structure is divergence and

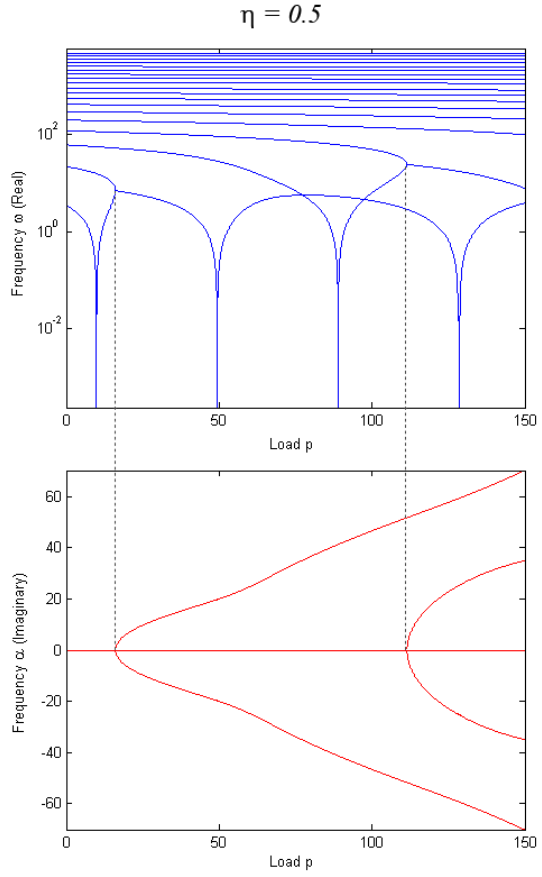

Figure 6: Load frequency curves for a load parameter of $\eta = 0.5$, representing the real and imaginary parts of the frequency values, obtained with the beam model.

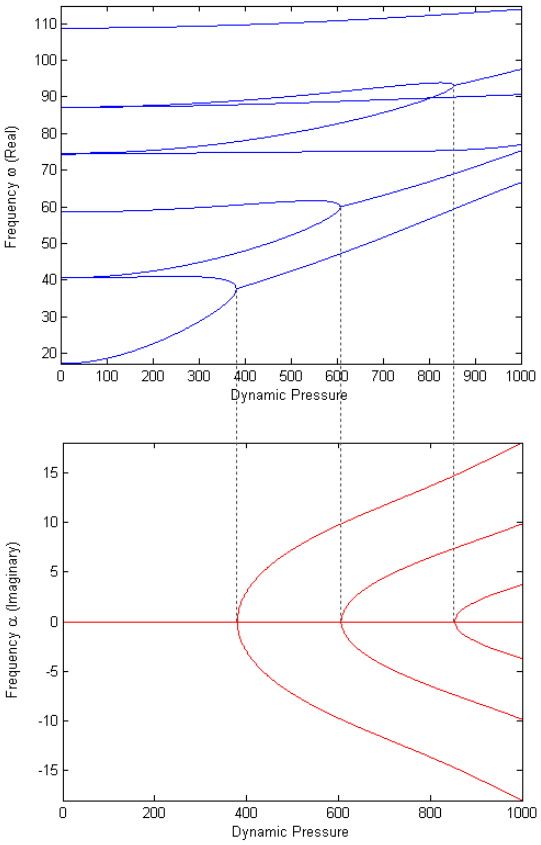

Figure 7: Dimensionless dynamic pressure as function of the frequency. Real (left plot) and Imaginary (right plot) representation.

$p_d = 9.870$. Notwithstanding, at this load condition flutter modes are also present. From the represented imaginary part of the frequency it is possible to identify two flutter modes. At the flutter load, while the real part of the two adjacent frequencies coalesce, their imaginary parts become non-zero and originate the two symmetric branches presented in the diagram. The first load occurs at a load of $p_f = 16.05$.

3.2 Stability Results for a Simply Supported Panel Under a Supersonic Flow

The stability analysis was implemented for a simply supported square panel, with 0.3×0.3 meters and a thickness of $0.01m$. These values are only relevant for the relative thickness with respect to the characteristic length of the plate, since all the results are presented in a dimensionless form.

The dimensionless dynamic pressure as a function of the frequency is presented in the two plots from figure 7, representing both the real and imaginary evolution of the critical dynamical pressure for the panel. Comparing these results with the results presented in figure 6, it is possible to recognize some similarities in the load frequency curves, especially in the complex domain, which reflect directly on the flutter mechanisms that originate such a structural response. When, for a certain dynamic pressure, flutter instability is reached, the load values enter the complex domain in the same way that when flutter occurred in the beam model, the frequency values presented two complex branches different from zero.

4 Optimization process

4.1 Problem Formulation

The purpose of the optimization method for the proposed models is to determine an optimal design which can allow the same stability boundaries as the original model. This problem can be presented

by,

$$\underset{\mu}{\text{Minimize}} \quad V \tag{20}$$

subject to,

1.Critical Load:	$p_{cr} \geq p_{cr}^0$
2.Frequency Curves:	$\lambda_{n+1} - \lambda_n \geq c$
3.Ensure Flutter Instability:	$\lambda_1 \geq 0$
4.Design Parameters:	$\mu_j^{min} \leq \mu_i \leq \mu_j^{max}$

where V is the dimensionless volume, p_{cr} is the dimensionless critical load, λ_n is the n^{th} dimensionless frequency and μ_i is the project variable at node i (which can be the equivalent dimensionless diameter or thickness, depending on the considered model).

The optimization algorithm for the beam formulation was implemented iteratively using the method of moving asymptotes developed and implemented in $MATLAB^{®}$ by Svanberg (1987). The iterative process stops when changes in the objective function are under 0.01% or when the iteration number reaches 150. In order to avoid large jumps in the design variables between iterations, limits where imposed. These limits were defined depending on the evolution of the optimization process, as well as the tuning parameters from MMA, which were also defined upon experience with the optimization algorithms.

4.2 Sensitivity Analysis

When implementing a structural optimization process using gradient based methods, it is necessary to perform a sensitivity analysis of the objective and constraint functions with respect to the design variables. The sensitivity analysis method for eigenvalue problems is fully described by Pedersen (2003). The sensitivities for the critical load, dynamic pressure and frequency values with respect to the design variables are given by:

$$\frac{\partial p_{cr}}{\partial \mu_j} = \frac{\mathbf{v}^T \left(\partial \mathbf{L}/\partial \mu_j\right) \mathbf{w}}{\mathbf{v}^T \left(\mathbf{G_c} - \eta \mathbf{G_f}\right) \mathbf{w}} \tag{21}$$

$$\frac{\partial Q_{cr}}{\partial \mu_j} = \frac{\mathbf{v}^T \left(\partial \mathbf{L}/\partial \mu_j\right) \mathbf{w}}{\mathbf{v}^T \mathbf{A} \mathbf{w}} \tag{22}$$

$$\frac{\partial \lambda}{\partial \mu_j} = \frac{\mathbf{v}^T \left(\partial \mathbf{L}/\partial \mu_j\right) \mathbf{w}}{\mathbf{v}^T 2\lambda \mathbf{M} \mathbf{w}} \tag{23}$$

and $\lambda = \omega$ for all $p < p_{cr}$, μ_e are the design variables, and $\mathbf{v}$ is the nodal solution vector of the problem adjoint to the finite element formulation presented by equation 19 and it is calculated solving the following algebraic equation,

$$\mathbf{L}^T \mathbf{v} = \left[\mathbf{K} - \lambda^2 \mathbf{M} + p\left(\mathbf{G_c} + \eta \mathbf{G_f}\right)\right]^T \mathbf{v} = 0, \tag{24}$$

where the values of p and λ correspond to the point for which the sensitivities are being calculated.

In the presented optimization problem, the objective function is the dimensionless structural volume, V, which for the beam model is calculated through a linear combination of the element lengths and nodal diameters as,

$$V = \mathbf{a}^T \mu, \quad \mathbf{a} = [l_1, l_1 + l_2, l_2 + l_3, \ldots, l_{N_e}] \tag{25}$$

where l are the element lengths and μ the project variables. For the plate model, the dimensionless volume is a linear combination of element lengths and heights with the nodal thickness, and is given by,

$$V = \sum_{j=1}^{N_{e_y}+1} \sum_{j=1}^{N_{e_x}+1} \mu_k b_i c_j, \qquad k = i + (j-1)(N_{e_x}+1) \tag{26}$$

with,

$$\begin{aligned} \mathbf{b} &= \left[l_{x_1}, l_{x_1} + l_{x_2}, l_{x_2} + l_{x_3}, \ldots, l_{x_{N_{e_x}}}\right] \\ \mathbf{c} &= \left[l_{y_1}, l_{y_1} + l_{y_2}, l_{y_2} + l_{y_3}, \ldots, l_{y_{N_{e_y}}}\right] \end{aligned}$$

where l_x is the element lengths in the x direction and l_y the lengths in the y direction. It is now possible to write the derivatives of the volume with respect to changes in the design variables as,

$$\frac{\partial V}{\partial \mu_j} = a_j \tag{27}$$

for the beam model and,

$$\frac{\partial V}{\partial \mu_k} = b_i c_j, \qquad k = i + (j-1)(N_{e_x}+1) \tag{28}$$

for the plate models. It should be noted that these derivatives are constant and do not depend on the design variables.

In order to verify the accuracy of the results from the analytical derivatives defined by 21, 22 and 23, they where compared with the numerical approximation given by the finite differences method. Using second-degree finite differences formulas to calculate the approximate solution for the derivatives, it was possible to obtain a very good agreement between analytical and numerical methods, with errors in the order of 10^{-6} %. This study confirms that the analytical expressions for the derivatives are accurate.

4.3 Optimization Results

4.3.1 Column Subjected to a Partial Non-Conservative End Load

This section presents the optimized structures obtained from the dimensionless uniform columns

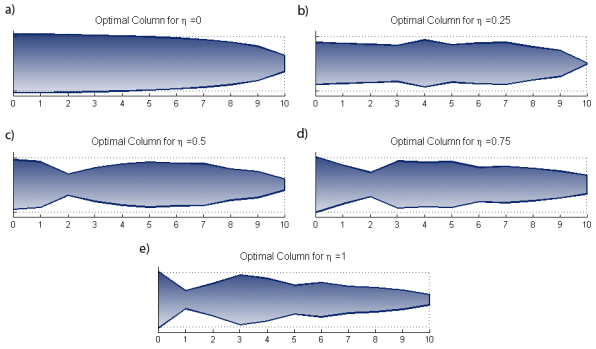

Figure 8: Optimized columns for various non-conservative load parameters. The dashed lines represent the uniform column.

with stability characteristics as presented in the previous section. A summary of the optimization results obtained for the five load conditions considered in the previous section is presented in the following table:

η	**0.00**	**0.25**	**0.50**	**0.75**	**1.00**
V_{opt}	0.866	0.476	0.473	0.490	0.374
ΔV (%)	13.4	52.4	52.7	50.9	62.6
Reference	0.866	–	0.486	–	0.379
Iterations	8	56	23	82	105

Table 1: Optimization results for the beam model.

These results were obtained using 3000 load steps for the stability analysis and 20 load points between 0 and p_{cr} for the calculus of the frequency sensitivities. The maximum and minimum values allowed for the design variables were selected as $\mu_{max} = 10$ and $\mu_{min} = 10^{-8}$, respectively.

As the results from the table show, the optimization process allowed for considerably large volume reductions while respecting all the imposed constraints. Comparing these results with the work presented by Langthjem and Sugiyama (2000a) once more, it is possible to verify that, for identical load conditions, the optimized results are lower, or equal at the worst, to the ones presented by these authors. Figure 8 shows the shape of the dimensionless optimized columns for the presented results.

4.3.2 Plate Subjected to a Partial Non-Conservative End Load

The optimization results presented in this section where obtained starting from the uniform dimensionless plate with the stability characteristics presented in the previous section. As for the beam model, a summary of the results is presented in the next table. Since the plate model was developed so as to have similar properties as the beam model, the optimized volumes obtained from the beam analysis are also presented,

η	**0.00**	**0.25**	**0.50**	**0.75**	**1.00**
V_{opt}	0.759	0.547	0.776	0.509	0.577
ΔV (%)	24.1	45.3	22.4	49.1	42.3
Iterations	42	32	44	46	33

Table 2: Optimization results for the cantilevered plate model.

In order to obtain the present results, several parameters had to be considered, as was the case for the beam model. The implied stability analysis algorithm used in the optimization process used 500 load steps and, once again, 20 load points between 0 and p_{cr}. The *MMA* tuning parameters where again upon experience, as for the previous analysis.

These results also allowed for considerable volume reductions, although the obtained volume values where higher than the presented values for the beam model. This was somewhat unexpected, but can possibly be justified by a series of reasons. First, the plate model takes into account the shear stresses on the structure and, as discussed by Langthjem and Sugiyama (2000a), this forces the thickness evolution along the plate to be smoother and, consequently inducing another limitation on the volume reduction. Another possible reason is the relatively small precision of the performed numerical calculus, both by the reduced number of elements used as well as the reduced number of load steps.

Figure 9 shows the evolution of the dimensionless thickness parameter. The darker tone indicated areas where material reinforcements are required, while lighter areas indicate that there is a reduced need of material in these areas.

4.3.3 Simply Supported Panel Under a Supersonic Flow

The optimization process developed for the minimization of the structural weight of a panel subjected to a low supersonic flow, follows the same basic considerations of the two previously presented models and some aspects relating the optimization of structures subjected to non-conservative loads were once again confirmed.

The need for frequency constraints in order to obtain a convergent optimization sequence is discussed with some level of detail by Odaka and Furuya (2005). They refer to the fact that when considering frequency separation in the optimization process we have a robust optimization scheme, because by ensuring this frequency separation, the

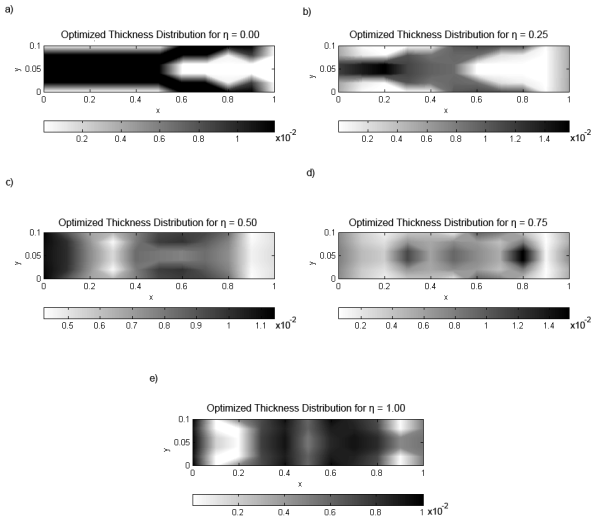

Figure 9: Optimized plate designs, showing the dimensionless thickness distribution for various non-conservative load parameters.

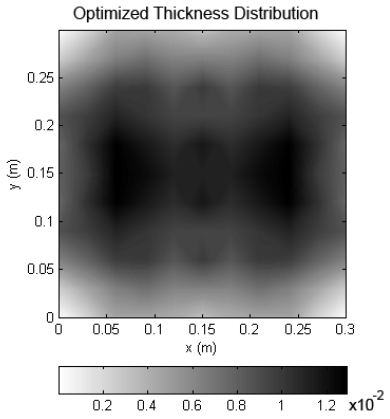

Figure 10: Dimensionless thickness distribution on the panel. Results obtained with a frequency separation constant of $c = 10$ and constraints on the project variables.

structure is optimized taking into account not only the main flutter instability mode, but also to higher modes. This robustness comes as a consequence of avoiding the mentioned convergence problems.

Considering now the frequency constraints in the optimization process it is possible to obtain a good convergence of the results in a relatively reduced number of iterations. Setting the frequency separation constant as $c = 10$, it is possible to obtain a volume reduction of 13.7%, with the thickness distribution represented in figure 10. These results were obtained with the project variables limited between $\mu_{max} = 1.5$ and $\mu_{min} = 0.5$ and a slack parameter set as $\epsilon = 0.1$.

5 Conclusions and Further remarks

From the work described in this article, it is possible to demonstrate the importance of finding optimal design solutions in flutter instability problems, since results show that it is possible to greatly reduce structural weight while maintaining structural stability. When considering applications like aeronautics, where structural weight and volume are an important design issue, large volume reductions as the ones obtained in the present work demonstrate the need for optimal solutions. It was possible to verify the well-known fact that flutter instability is very sensitive to shape and load variations.

From the first implemented model, it is possible to verify one of the basic characteristics of structural optimization problems: When a structure is optimized for a certain load condition, it's behavior when subjected to loading conditions different from the project load will be affected. The implemented beam model was tested for several different load conditions, reproducing results available in the bibliography for both the stability analysis and optimization methods.

It is also important to keep in mind that the obtained optimization results for the plate and panel flutter models are preliminary and where obtained while writing the current thesis. Since the optimization process depends upon a large number of factors that must be adjusted according to the developers experience and sensitivity to the problem at hand, it is likely that further work will produce better results.

As further work to be developed, it is possible to point out the verification of the developed models with any available reference examples and data, or even developing experimental verification models. The development of the analysis algorithms using different theoretical principles, such as considering the beam formulation by the Timoshenko beam and a Kirchhoff plate formulation. These verifications would ensure the robustness and accuracy of the developed models. The implementation of new optimization approaches to the problem would also be greatly valued, as well as a study on the influence of the different optimization parameters on the final optimized results. Finally, the generalization of the developed models for more realistic and complex structural models would be an excellent follow up for the present work.

6 Acknowledgements

I am thankful to my supervisor, professor Miguel Matos Neves, and co-supervisor, professor Afzal Suleman, for their support and dedication for the development of this thesis. I am also grateful to Prof. Krister Svanberg from Royal Institute of Technology, Stockholm, for providing his *MATLAB*® version of MMA. This work received support from FCT through the project POCTI/EME/ 44728/2002 (MMN), FEDER and IDMEC-IST and CAPS-UFSC (Brazil).

References

I Elishakoff. Controversy associated with the so-called 'Follower Forces': Critical overview. *Transactions of the ASME*, 58:117–142, 2005.

G. Jayaraman and A. Struthers. Divergence and flutter instability of elastic specially orthotropic plates subject to follower forces. *Journal of Sound and Vibration*, 281:357–373, 2005.

J. H. Kim and J. H. Park. On the dynamic stability of rectangular plates subjected to intermediate follower forces. *Journal of Sound and Vibration*, 209(5):882–888, 1998.

J. S. Kim and H. S. Kim. A study on the dynamic stability of plates under a follower force. *Computers and Structures*, 74:351–363, 2000.

M. A. Langthjem and Y. Sugiyama. Optimum design of cantilevered columns under the combined action of conservative and nonconservative loads, part 1: The undamped case. *Computers and Structures*, 74:385–398, 2000a.

M. A. Langthjem and Y. Sugiyama. Optimum design of Beck's column with a constraint on the static buckling load. *Structural Optimization*, 18: 228–235, 1999.

M. A. Langthjem and Y. Sugiyama. Dynamic stability of columns subjected to Follower Loads: A survey. *Journal of Sound and Vibration*, 238(5): 809–851, 2000b.

M. A. Langthjem, Y. Sugiyama, and B. J. Ryu. Letters to the editor: Realistic Follower Forces. *Journal of Sound and Vibration*, 225(4):779–782, 1999.

Y. Odaka and H. Furuya. Robust structural optimization of plate wing corresponding to bifurcation in higher mode flutter. *Structural Multidisciplinary Optimization*, 30:437–446, 2005.

P. A. C. Pastilha. Structural optimization for flutter instability problems. Master's thesis, Instituto Superior Técnico, 2007.

P. Pedersen. *Optimal Designs - Structures and Materials - Problems and Tools*. draft, May 2003.

J. N. Reddy. *Introduction to the finite element method*. McGraw-Hill Publishing Co., 1992. ISBN 0-07-113210-4.

Y. Sugiyama, K. Katayama, K. Kiriyama, and B. J. Ryu. Experimental verification of dynamic stability of vertical cantilevered columns subjected to a sub-tangential force. *Journal of Sound and Vibration*, 236(2):193–207, 2000.

Y. Sugiyama, S. U. Ryu, and M. A. Langtjem. Beck's column as the ugly duckling. *Journal of Sound and Vibration*, 254(2):407–410, 2002.

A. Suleman and M. A. Gonçalves. Optimization issues in application of piezoelectric actuators in panel flutter control. *SPIE 4th Annual Symposium on Smart Structures and Materials*, 1997.

A. Suleman and V. B. Venkayya. Formulation of a composite panel with piezoelectric layers for application to the panel flutter problem. *IUTAM Symposium on The Active Control of Vibration*, 1994.

A. Suleman and V. B. Venkayya. Flutter control of an adaptive laminated composite panel with piezoelectric layers for application to the panel flutter problem. *AAIA/USAF/NASA/ISSMO Symposium on Multidisciplinary Analysis and Optimization*, 1996.

K. Svanberg. The Method of Moving Asymptotes - a new method for structural optimization. *International Journal for Numerical Methods in Engineering*, 24(2):359–373, 1987.

K. H. Zuo and H. L. Schreyer. Flutter and divergence instability of nonconservative beams and plates. *Int. J. Solids Structures*, 33(9):1355–1367, 1996.